Electronic Supplementary Material (ESI) for Reaction Chemistry & Engineering.

Supporting Information:

Understanding Electrochemically Induced Olefin Complexation: Towards Electrochemical Olefin-Paraffin Separations

---

Table of Contents

Section S1: H-NMR Multiplicity and Experimental Confirmation 3
Section S2: Electrochemical H-Cell Reactor 5
Section S3: Equilibration Time of Complexation Reaction 6
Section S4: Complexation Equilibrium Constant 7
Section S5: Decomplexation of 1-pentene from $[Ni(IV)(mnt)_2]^0 \cdot C_5H_{10}$ 8
Section S6: Oxidative Conversion of $[Ni(II)(mnt)_2]^{2-}$ at varying concentrations and current densities 9

Section S1: H-NMR Multiplicity and Experimental Confirmation

H_A is expected to be a quartet of doublet because it has 1 neighboring hydrogen (i.e., H_B), is diastereostopic, and is attached to a chiral carbon. H_B is a quintet simply because it has 4 neighboring hydrogen atoms. Chemical shifts were located at 4.75 and 3.68 ppm for H_A and H_B, respectively. The chemical shifts for the remaining hydrogen atoms of 1-pentene overlapped with chemical shifts of other known compounds, so they were not pursued as main chemical shifts of interest for olefin-complex quantification. Additionally, the integral area of the H_A vs. H_B peaks was approximately a ratio of 2, further supporting the identity of the chemical shift as belonging to the complexed 1-pentene molecule (because there is 2 H_A for every 1 H_B). For many of the subsequent experiments, H_A's chemical shift was utilized to quantify the concentration of the $Ni(mnt)_2^0 \cdot C_5H_{10}$ complex because its unique quartet of doublet signal was easier to locate and integrate. The mole fraction of the available $[Ni(mnt)_2]^0$ that complexed with 1-pentene is the ***Olefin-Capture UF***. Also, note that the unbound state of 1-pentene (as shown in the peaks marked as excess 1-pentene in **Figure S1**) and the bound state of 1-pentene are at different chemical shifts and are therefore not of the same single molecular structure.

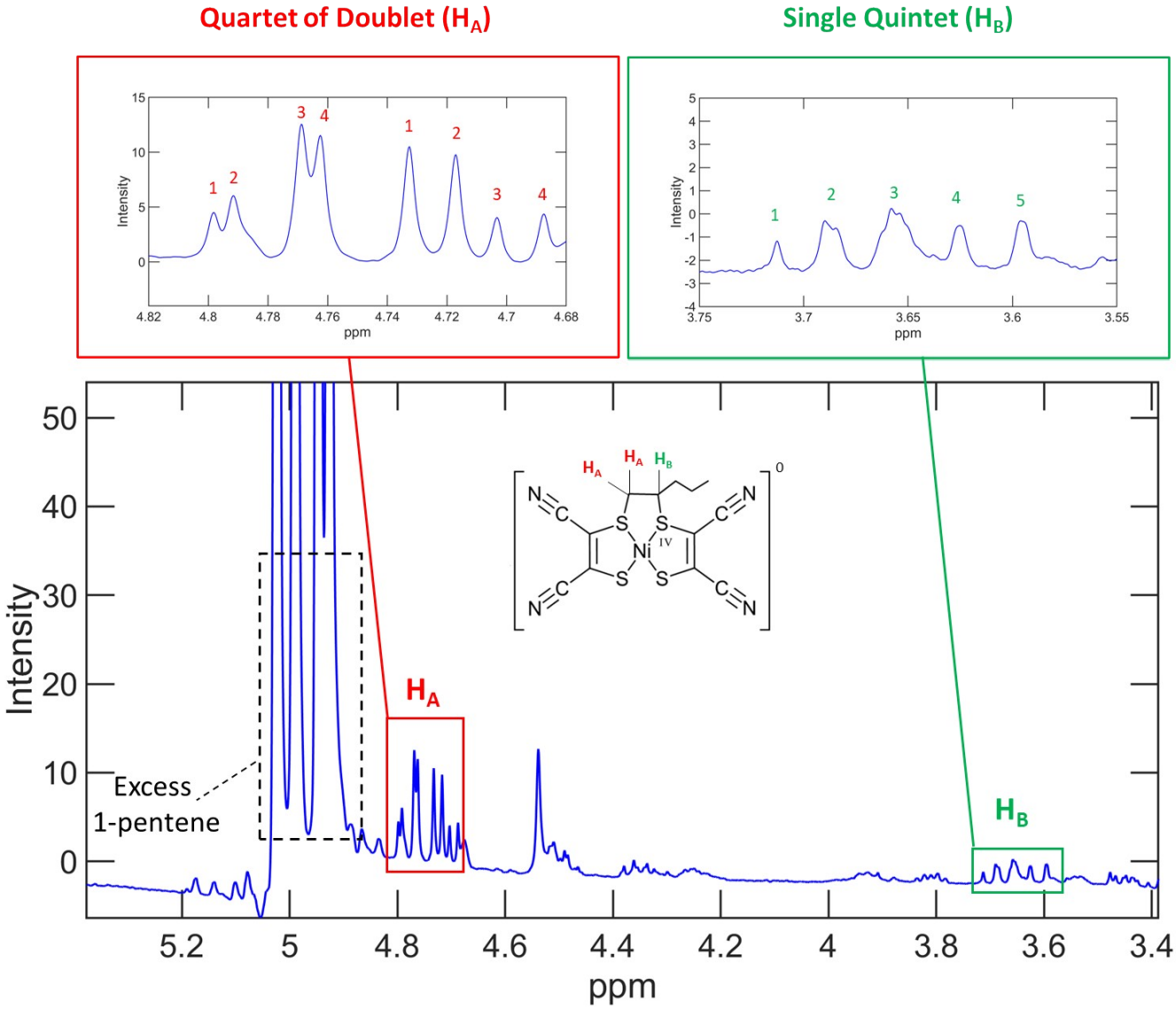

Figure S1. H-NMR plot of $[Ni(mnt)_2]^0 \cdot C_5H_{10}$ containing solution after oxidation is shown. Two unique sets of chemical shifts were utilized to verify that the peaks belonged to the complexed 1-pentene molecule attached to the $[Ni(mnt)_2]^0$ species. 10 mM of tetrabutylammonium Ni(II) maleonitriledithiolate was prepared in a 99.9% deuterated acetonitrile solution with saturated lithium nitrate as supporting electrolyte. A reaction solution of 16 ml underwent constant-current chronopotentiometry of 5 mA for 100 minutes. 500 µl of the reaction solution was directly extracted from the H-cell reactor for H-NMR analysis.

Section S2: Electrochemical H-Cell Reactor

The Electrochemical H-Cell Reactor is made up of many interchangeable parts to allow improved modularity for possible new designs to complement the reactor. The core parts, especially those that would encounter chemical solutions, are made of Teflon for chemical resilience. The reactor can have a tightly sealed lid secured by screw bolts and hex nuts for experiments where exposure of organic volatiles to air needs to be controlled. The reactors are periodically disassembled and cleaned between experimental trials. The lids also help secure the electrodes to be in place so that they do not drastically change position, especially during electrochemical modulation steps, so that the current and potential are not disturbed.

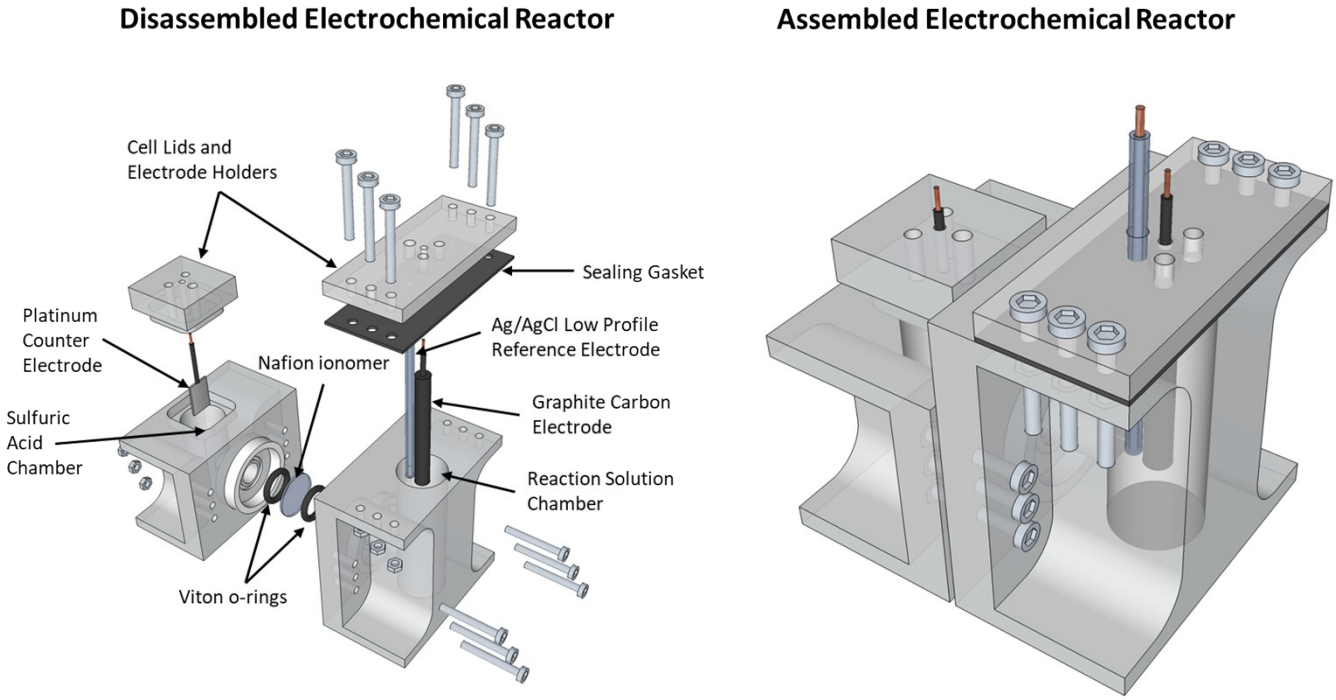

Figure S2. Electrochemical Cell utilized in the experiment was made of Teflon material to be compatible with acetonitrile solution used in the reaction solution. It is also a divided cell, allowing oxidation to occur exclusively in the reaction solution without worrying about reduction reaction on the counter side. The pieces are tightly assembled with stainless steel screws and hex nuts. The cell lid on the working side (reaction solution chamber) consists of holes that can be plugged to reduce air exposure. Whenever a sample solution needs to be extracted, a syringe needle is pierced through the septum cap to carefully remove the solution under a controlled environment.

Section S3: Equilibration Time of Complexation Reaction

Time-dynamic measurements spanning 72 hours of elapsed complexation and equilibration time were made to observe the amount of time needed for the complex to reach equilibrated state so that an accurate equilibrated concentration of $[Ni(mnt)_2]^0 \cdot C_5H_{10}$ can be measured via H-NMR. The following combinations of initial concentrations of $[Ni(mnt)_2]^{2-}$ and 1-pentene were utilized to observe the concentration profile of $[Ni(mnt)_2]^0 \cdot C_5H_{10}$ complex.

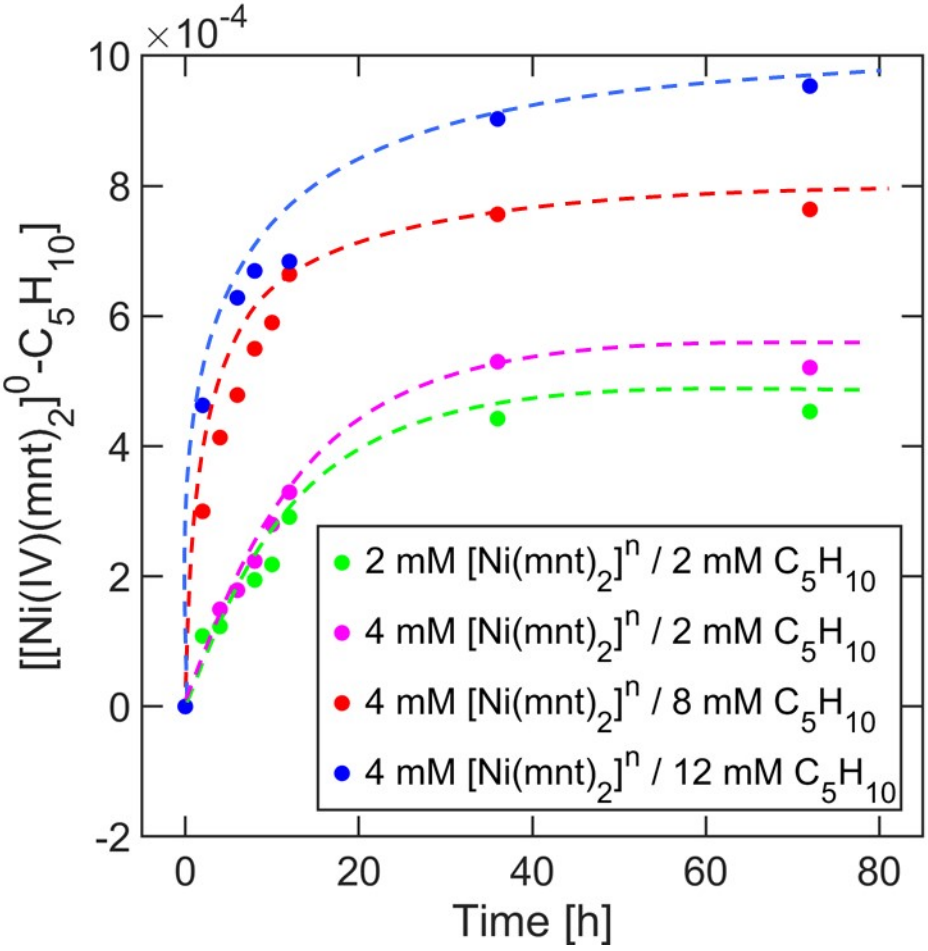

Figure S4. The long-term concentration profile above shows the concentration of $[Ni(IV)(mnt)_2]^0 \cdot C_5H_{10}$ complex gradually reaching asymptotic slopes representing the equilibrium state of the reaction. The equilibrium constant, K_{eq}, can be determined for all experiments done in Section 2 because 72 hours was given for the reactant species to complex, more than enough time to reach equilibrium condition. The 4 combinations of initial concentration conditions are shown in the legend embedded in the above figure.

Section S4: Complexation Equilibrium Constant

K_{eq} was calculated for each distinct experimental condition analyzed for observed the trends discussed in **section 3** of the main manuscript. The constants were then averaged and that average K_{eq} was then used to make a theoretical UF plot for varying 1-pentene and varying $[Ni(II)(mnt)_2]^{2-}$ concentration trends in **Figure 4B** and **5C** of the manuscript.

Current Density [mA/cm^2]	Initial Concentration [mM]			Equilibrated Concentration [mM]			K_{eq} [M^{-1}]
	$[Ni(II)(mnt)_2]^{2-}$	C_5H_{10}	$[Ni(IV)(mnt)_2]^0 \cdot C_5H_{10}$	$[Ni(IV)(mnt)_2]^0$	C_5H_{10}	$[Ni(IV)(mnt)_2]^0 \cdot C_5H_{10}$	
0.57	5	5	0	4.67	4.67	0.33	**15.11**
0.57	5	25	0	3.78	23.78	1.22	**13.55**
0.57	5	50	0	3.66	48.66	1.34	**7.53**
0.57	5	100	0	2.40	97.40	2.60	**11.16**
0.57	10	100	0	4.92	94.92	5.08	**10.89**
0.57	15	100	0	8.54	93.54	6.46	**8.09**
0.57	20	100	0	12.94	92.94	7.06	**5.87**
0.11	5	100	0	2.43	97.43	2.57	**10.84**
0.23	5	100	0	2.61	97.61	2.39	**9.41**
0.34	5	100	0	2.54	97.54	2.46	**9.91**
0.8	5	100	0	2.56	97.56	2.44	**9.78**
						Average:	**10.20**
						Standard Deviation:	**2.61**

Table S4. All electrochemical and concentration parameters for initial and final equilibrated state are shown in the above table. K_{eq} was calculated for each set of conditions on the right-hand column, with the average and standard deviation values shown towards the bottom.

Section S5: Decomplexation of 1-pentene from $[Ni(IV)(mnt)_2]^0 \cdot C_5H_{10}$

Decomplexation of 1-pentene was attempted for $[Ni(IV)(mnt)_2]^0 \cdot C_5H_{10}$ generated post-oxidation from a starting reaction condition of 5 mM $[Ni(II)(mnt)_2]^{2-}$and100 mM 1-pentene in saturated lithium nitrate acetonitrile solution. The mixture was applied with enough oxidative charge to convert all of the $[Ni(II)(mnt)_2]^{2-}$ present in the solution via constant positive current density of 0.57 mA/cm^2 for approximately 50 minutes. The reaction solution was then given at least 3 days to reach equilibration point, allowing maximum complexation to occur. Next, the solution was applied a constant reductive current of -0.57 mA/cm^2 for approximately 200 minutes to reduce the oxidation state of Ni from IV to II, in order to decouple the complexed 1-pentene off from $[Ni(II)(mnt)_2]^{2-}$. The appearance of the unique quartet of doublet peak after oxidation and the subsequent decline of the same peak after reduction demonstrates that both the oxidative capture and reductive release of olefin can be characterized and quantified in the liquid reactor electrochemical cell.

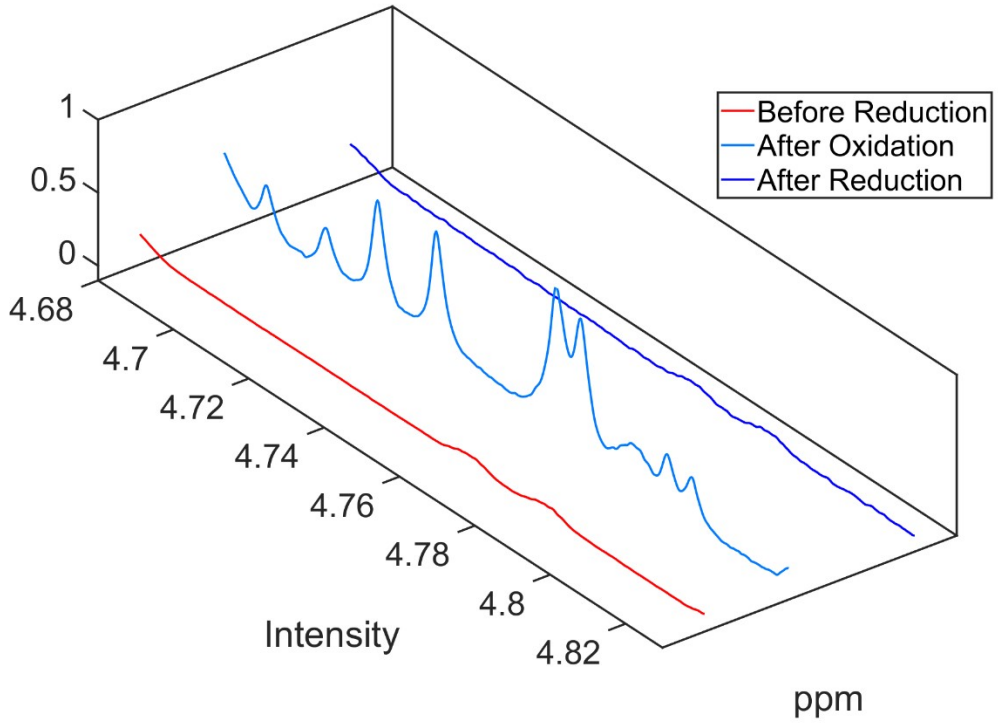

Figure S5. The NMR spectra above depicts the unique quartet of doublet peak appearing and disappearing after complexation, and after decomplexation, induced by electrochemical oxidation and reduction, respectively.

Section S6: Oxidative Conversion of $[Ni(II)(mnt)_2]^{2-}$ at varying concentrations and current densities

In **Figure 6** of the main article, it was shown that current density did not play a significant role in influencing the UF and therefore the conversion rate of $[Ni(II)(mnt)_2]^{2-}$. To further supplement the observation that current density is decoupled from conversion rate, a series of experiments was conducted to demonstrate how the conversion rate of $[Ni(II)(mnt)_2]^{2-}$ was not influenced at different initial concentrations of $[Ni(II)(mnt)_2]^{2-}$ at constant 1-pentene concentration of 100 mM in acetonitrile solution saturated with lithium nitrate as supporting electrolyte. In each experiment, a stoichiometric amount of oxidative charge was applied to convert all of the $[Ni(II)(mnt)_2]^{2-}$ present in the solution, regardless of current density and then the solution was characterized by UV-Vis spectroscopy to observe the effect on the conversion rate of $[Ni(II)(mnt)_2]^{2-}$. **Figure S6** depicts how the conversion rate behaves similarly to other experimental conditions (shown in **Figure 3** of the main article), showing the disappearance of key absorbance peaks after applying oxidative current to the reaction solution. Regardless of the current density and initial concentration of $[Ni(II)(mnt)_2]^{2-}$, the electrochemical oxidation step in the olefin capture cycle appears to be very efficient.

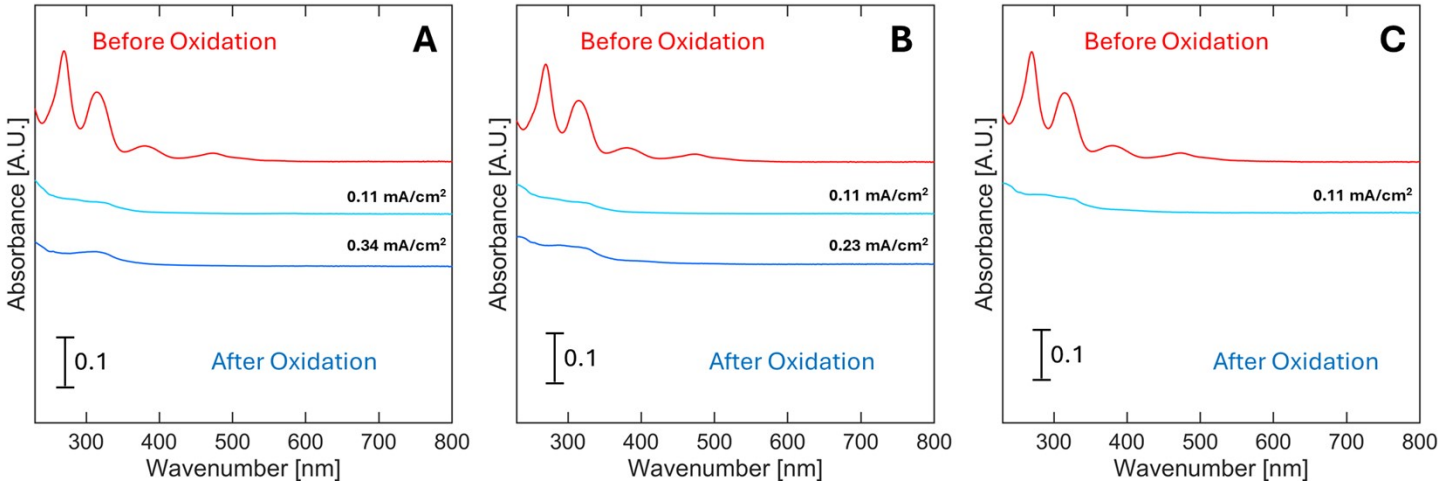

Figure S6. Varying current densities were applied to three different starting concentrations of $[Ni(II)(mnt)_2]^{2-}$ as shown in the UV-Vis absorbance spectra above. 10, 15, and 20 mM $[Ni(II)(mnt)_2]^{2}$ were used in A, B, and C, respectively, at a constant 100 mM 1-pentene concentration in acetonitrile solution saturated with lithium nitrate. To achieve equivalent charge to each experimental condition, reaction time was adjusted depending on the initial moles of $[Ni(II)(mnt)_2]^{2-}$ present in the reaction mixture and the current being applied to the system. In all experiments shown in A, B, and C, the absorbance peaks of Ni(II) are visibly conspicuous before oxidation, but diminishes after oxidation regardless of the magnitude of applied current densities.